IEICE TRANS. COMMUN., VOL.E102–B, NO.11 NOVEMBER 2019

PAPER

Enhanced Selected Mapping for Impulsive Noise Blanking in Multi-Carrier Power-Line Communication Systems

Tomoya KAGEYAMA[†a)], ***Student Member***, **Osamu MUTA**[†b)], ***and*** **Haris GACANIN**[††], ***Senior Members***

SUMMARY In this paper, we propose an enhanced selected mapping (e-SLM) technique to improve the performance of OFDM-PLC systems under impulsive noise. At the transmitter, the best transmit sequence is selected from among possible candidates so as to minimize the weighted sum of transmit signal peak power and the estimated receive one, where the received signal peak power is estimated at the transmitter using channel state information (CSI). At the receiver, a nonlinear blanking is applied to hold the impulsive noise under a given threshold, where impulsive noise detection accuracy is improved by the proposed e-SLM. We evaluate the probability of false alarms raised by impulsive noise detection and bit error rate (BER) of OFDM-PLC system using the proposed e-SLM. The results show the effectiveness of the proposed method in OFDM-PLC system compared with the conventional blanking technique.

key words: *power-line communications (PLC), OFDM, impulsive noise blanking, peak-to-average power ratio (PAPR), selected mapping (SLM)*

1. Introduction

Powerline communications (PLC) has been widely investigated to enable high speed home applications over existing power lines [1]. Since, the electric power lines were not originally designed for wideband transmissions the received signal is severely distorted due to impulsive noise channel characteristics [2]–[5]. In PLC systems, mitigating the impulsive noise by techniques such as deliberate blanking is important for enhancing the transmission performance further. However, since multi-carrier PLC signals exhibit high peak-to-average power ratio (PAPR) values [6], which degrades the accuracy of impulsive noise detection. More accurately, in OFDM-PLC, the receiver may remove not only impulsive noise but also signal samples which exceeds the blanking threshold. As a result, BER performance is degraded due to misdetection of impulsive noise on the receiver side. To improve the transmission performance, the peak amplitude of the received signal has to be reduced below the blanking threshold. However, even if the peak amplitude of the OFDM signal is suppressed on the transmitter side, PAPR of the received signal may not be suppressed, because multi-path signals are combined at the receiver side since triggering peak amplitudes may regrow at the receiver. This motivates us to consider reducing the PAPR of received signal. The target of this paper is OFDM-PLC system using deliberate blanking in presence of impulsive noise.

In this paper, we propose an enhanced selected mapping (e-SLM) technique for joint transmit/receive peak amplitude reduction for OFDM-PLC systems with impulsive noise blanking, where the transmitter selects the best transmit sequence among possible candidates so as to optimize PAPR characteristics of both transmit signal and receive signal, provided that CSI is available on the transmitter side. In the proposed e-SLM, the weighted sum of peak power of transmit signal and the estimated peak power of the received signal is used as a metric to optimize their PAPR characteristics. On the receiver side, a deliberate blanking is applied to mitigate the influence of impulsive noise, where the received values exceeding a given threshold are blanked as impulsive noise. Main features of this paper are summarized as follows*:

- Unlike conventional approaches using the blanking technique, e-SLM presented in this paper is effective in mitigating both power amplifier nonlinearity and the influence of impulsive noise.
- Since end-to-end performance of SLM highly depends on channel estimation (CE) accuracy, we present an iterative CE method for e-SLM. The estimated CSI is utilized to optimize PAPR of both transmit and received signals at the transmitter side. The proposed CE method is designed based on mean square error (MSE) criteria to estimate the efficient channel impulse response (CIR) and reduce the negative effect of noise, where an adaptive windowing technique is adopted to improve channel estimation accuracy.
- This paper discusses BER performance of OFDM-PLC system in both mathematical channel model and measured channel models to clarify the effect of e-SLM with the iterative CE.

2. Related Works

Impulsive noise suppression techniques such as blanking and clipping have been investigated for PLC systems in literature [8]–[15]. In particular, various performance analyses of OFDM systems with blanking based impulsive noise reduction techniques are presented such as in [8]–[12]. In these works, it is analyzed that output signal-to-noise power ratio

Manuscript received April 2, 2019.
Manuscript publicized May 16, 2019.

[†]The authors are with Kyushu University, Fukuoka-shi, 819-0371 Japan.
[††]The author is with Nokia Bell Labs, Belgium.
a) E-mail: kageyama@mobcom.ait.kyushu-u.ac.jp
b) E-mail: muta@m.ieice.org

DOI: 10.1587/transcom.2019EBP3081

*This work was presented in part at the 2018 IEEE International Symposium on Power Line Communications and its Applications (IEEE ISPLC2018) in [7].

(SNR) can be maximized by selecting the optimum impulsive noise detection threshold. However, in the above works, PAPR of OFDM signal is not taken into account. To further improve the system performance, minimization of PAPR is required.

To solve this issue, PAPR reduction techniques such as partial transmit sequence (PTS) [16], selected mapping (SLM) [17], [18], and companding [19], constant envelope OFDM (CE-OFDM) [20], [21] are applied to OFDM-PLC system so as to mitigate nonlinear distortion due to blanking at the receiver. In, [17], both SLM and blanking are applied to OFDM-PLC system to improve output SNR in impulsive noise channel. Work in [19] represents that a companding based technique is applied to the transmitter side in order to reduce peak power of the transmit signal and theoretical analysis of achievable performance. In [21], CE-OFDM technique [20] is investigated to improve output SNR at the receiver with impulsive noise blanking. However, the above works focus on only the peak amplitude reduction of the transmit signal and peak amplitude regrowth at the receiver side is not taken consideration, i.e., even if peak amplitude of the transmit signal is reduced, the peak amplitude of the receive signal is not kept to a low value, because multi-path signals are combined at the receiver and thus high peak amplitude regrowth occurs. Therefore, it is required to keep the peak amplitude of both transmit and received signals below a certain value. To solve this problem, it is necessary to consider PAPR reduction of the received signal passing through multi-path PLC channels in presence of impulsive noise.

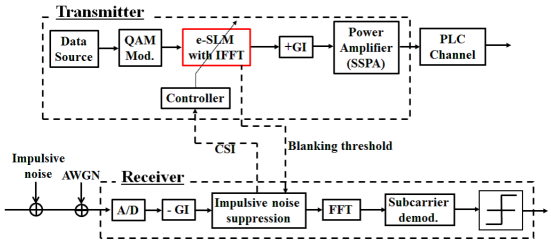

(a) PLC system model.

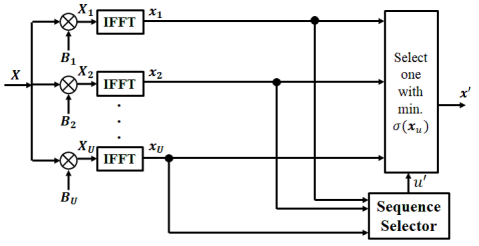

(b) Block diagram of e-SLM.

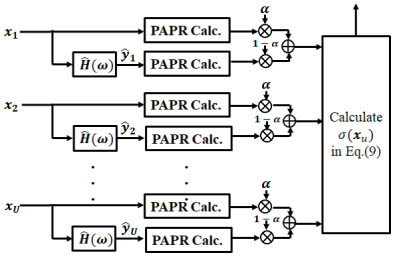

(c) Sequence selector.

Fig. 1 The block diagram of OFDM-PLC systems using the proposed e-SLM and impulsive noise blanking.

3. E-SLM OFDM-PLC System

3.1 System Description

Figure 1(a) shows a block diagram of OFDM-PLC system considered in this paper. On the transmitter side, the data sequence is modulated with the QAM technique. After that, OFDM modulation is carried out with inverse fast Fourier transform (IFFT). In addition, the proposed e-SLM scheme is applied to minimize the peak power of both transmit and receive signals. The details of the proposed e-SLM are explained in Sect. 4. A guard interval (GI) is added to each OFDM symbol in order to avoid inter-symbol interference. The transmit signal is amplified at the power amplifier (PA). In this study, we introduce a solid-state power amplifier (SSPA) model whose input-output function is given as $|y(t)| = \beta|x(t)|/\left[1+\left(|x(t)|/\sqrt{P_{sat}}\right)^{2p}\right]^{\frac{1}{2p}}$, where p=4 is assumed as a typical value to examine the influence of nonlinear PA. In this model, input-back-off (IBO) is defined as the average power of the input signal (P_{ave}) normalized by a reference power (P_{sat}) that corresponds to a saturation level. IBO in dB is given as $10\log_{10}(P_{ave}/P_{sat})$, where β denotes the gain of the amplifier and we assume $\beta = 1$ in this paper for simplicity of discussions.

On the receiver side, an analog-to-digital converter (ADC) is used to digitize the analog signals, where in-phase and quadrature components of the input signal are quantized uniformly with 2^Q quantization levels, respectively. The maximum output level is denoted as V_{max}: dynamic range of ADC is given as $D_R = 10\log_{10}((2V_{max})^2/P_a)$ in dB, where P_a denotes the average power of the signal. After A/D conversion and GI removal, the blanking is applied to mitigate the influence of impulsive noise. Finally, the received signal is demodulated with an FFT to detect the data.

3.2 Channel Model

3.2.1 Analytical Model

Figure 2(a) shows the two-branch PLC channel topology used in this paper. We assume that the reflection between E and F is negligible so that the total transfer function of two branch channel model is approximated as two independent T-topology networks [22]–[24]. In Fig. 2(a), the transmitter and the receiver are located on node A and B, respectively. For simplicity of discussion, we also assume that node C and node D are left open and impedance matching between A and B is attained. Based on these assumptions, two-branch channel topology in Fig. 2(a) can be treated as cascaded two independent T-topology channel. The maximum number of reflections at C and D is limited to N_r. Figure 2(b)

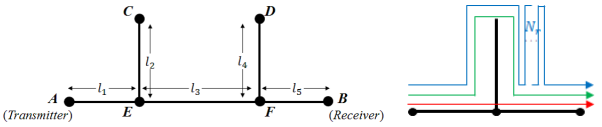

(a) Two-branch PLC channel topology. (b) Single T-topology.

Fig. 2 PLC channel topology.

shows single T-topology channel, where N_r=2 is assumed. As shown in this figure, in each T-topology channel, since direct path and N_r reflected paths appear, the total number of paths is N_r+1. Thus, when x independent T-topology channels are cascaded, the total number of paths is given as $(N_r + 1)^x$. In this paper, we consider two-cascaded channel (x=2) and assume N_r=1 (i.e., the total number of path is 4). The reflections at each branch end construct a multipath channel, where the frequency-transfer function is given as

$$H(f) = \sum_{i=1}^{(N_r+1)^2} g_i \cdot e^{-\mathrm{Re}[\gamma(f)]d_i} e^{-j\mathrm{Im}[\gamma(f)]d_i}, \quad (1)$$

where d_i and g_i denote the length and the attenuation coefficient of the i-th path [23], respectively. $\gamma(f)$ represents the propagation coefficient of the channel defined as

$$\gamma(f) = \sqrt{\frac{(R + j2\pi fL)}{(G + j2\pi fC)}}, \quad (2)$$

where R, L, G and C denote resistance, inductance, conductance and capacitance of the transmission line, respectively. In this paper, the above parameters for unit length (1 meter) metal cable (copper cable) are given as $R = \frac{1.15\rho}{\pi\delta(2r_0-\delta)}[\Omega]$, $C = 50[pF]$, $L = 0.5[\mu H]$ and $G = 0.63[S]$, respectively. Here, electrical resistance ρ, skin depth δ, radius of copper line r_0 are respectively given as $r_0 = 0.511 \times 10^{(3/2)}$, $\delta = \sqrt{2\rho/(4\pi\omega \times 10^{-7})}$, $\rho = 1.72 \times 10^{-8}$ and $\omega = 2\pi f$, where f denotes frequency[†].

3.2.2 Measured Channel

Figure 3 illustrates channel frequency measurements under impulsive noise environment in two different time instances. To measure these power line characteristics, we constructed an indoor PLC network using three modems to measure power line characteristics. One laptop PC is connected to one of the modems to measure data. Channel measurement results in Fig. 3 are obtained by two different time instances, where solid line and dotted line are referred as "Measured channel I" and "Measured channel II", respectively. We assume that phase characteristic of the channel is ideal, i.e., the frequency response is given as,

$$H_{meas} = |H_m(f)| \exp(2\pi fT), \quad (3)$$

where $|H_m(f)|$ represents the measured frequency gain of PLC channel.

[†]Parameters in $\gamma(f)$ are experimentally obtained.

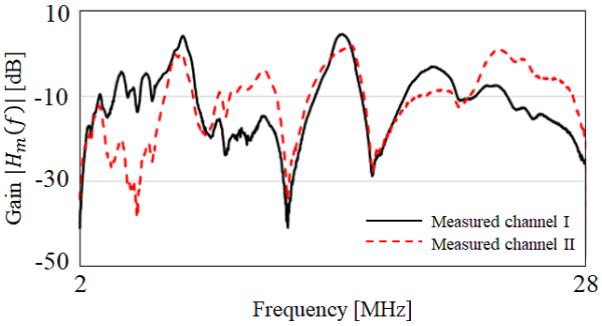

Fig. 3 Measured frequency response of a PLC channel.

3.3 Impulsive Noise Model

Middleton's Class-A impulsive noise model [25]–[26] is used. Class-A noise amplitude is expressed as

$$n_A(t) = n_W(t) + n_I(t),$$

where $n_W(t)$ and $n_I(t)$ denote AWGN and impulsive noise, respectively. In this model, probability of occurrence of impulsive noise follows a Poisson distribution, while probability density function (PDF) of impulsive noise amplitude $n_I(t)$ follows a Gaussian distribution with zero-mean and variance $\frac{\sigma_I^2}{A}$. Let σ_W^2 and σ_I^2 denote the variance of $n_W(t)$ and that of $n_I(t)$, respectively. Here, $\Gamma = \frac{\sigma_W^2}{\sigma_I^2}$. Note that higher impulsive noise appears when Γ is smaller value. Assuming that probability of occurrence of impulsive noise follows a Poisson distribution with mean value of $A = r_i T_s$, the PDF of Class-A noise amplitude is given as follows:

$$f(x) = e^{-A} \sum_{k=0}^{\infty} \frac{A^k}{k!\sqrt{2\pi\sigma_k^2}} \exp\left(-\frac{x^2}{2\sigma_k^2}\right), \quad (4)$$

where r_i and T_s denote the number of impulsive noise occurrence per unit-time and OFDM symbol duration, respectively. Here, $\sigma_k^2 = \frac{k/A+\Gamma}{1+\Gamma}$. In Eq. (4) as A increases, the probability of impulsive noise occurrence increases while the magnitude of impulsive noise decreases.

4. E-SLM for OFDM-PLC System with Impulsive Noise Blanking

4.1 e-SLM at the Transmitter Side

The block diagram of OFDM-PLC system using the proposed e-SLM and impulsive noise blanking is shown in Fig. 1. The proposed e-SLM works so as to minimize the weighted sum of the PAPR of the transmit signal and estimated PAPR of the received signal. We assume that channel state information (CSI) is available on the transmitter side. In the e-SLM, the original data sequence $\mathbf{X} = [X_0, X_1, ..., X_{L-1}]^T$ is scrambled with U different random phase sequences $\mathbf{B}_u = [b_{u,0}, b_{u,1}, ..., b_{u,L-1}]$

$(u = 1, 2, ..., U)$, where $\mathbf{X}$, $\mathbf{B}_u \in \{0, 1\}^L$, and L denotes the number of subcarriers. The u-th candidate data vector $\mathbf{X}_u = [X_{0,u}, X_{1,u}, ..., X_{L-1,u}]$ is expressed as

$$\mathbf{X}_u = \mathbf{X} \oplus \mathbf{B}_u, \tag{5}$$

where $\oplus$ denotes element-by-element modulo-2 addition. $\mathbf{X}_u$ is transformed to time domain signal vector. $\mathbf{x}_u \equiv \text{IFFT}[\mathbf{X}_u]$ by inverse fast Fourier transform (IFFT). Let $\hat{\mathbf{H}} = \text{diag}(\hat{H}_1, \hat{H}_2, ..., \hat{H}_L)$ denote the estimated CSI. For simplicity of discussion, in this paper, we assume that estimated CSI is ideally informed to the transmitter side. The estimated (replicated) received signal $\hat{\mathbf{Y}}_u = [Y_{0,u}, Y_{1,u}, ..., Y_{L-1,u}]$ is given as

$$\hat{\mathbf{Y}}_u = \hat{\mathbf{H}}\mathbf{X}_u, \tag{6}$$

where the u-th time domain estimated received signal $\hat{\mathbf{y}}_u$ can be expressed as $\hat{\mathbf{y}}_u = \text{IFFT}[\hat{\mathbf{Y}}_u]$. Let $P_a(\mathbf{a})$ be a function that outputs the normalized maximum value of elements contained in vector $\mathbf{a}$.

$$P_a(\mathbf{a}) = \frac{\|\mathbf{a}\|_\infty^2}{E[\|\mathbf{a}\|_2^2]}, \tag{7}$$

where $E[\cdot]$ denotes the expectation operation and $\|\cdot\|_b$ represents the b-norm. The transmitter selects the best sequence $\mathbf{x}' = \mathbf{x}_{u'}$ which minimizes the weighted sum of peak amplitude of the candidate transmitted signal and its estimated received signal;

$$u' = \arg\min_{1 \le u \le U} \sigma(\mathbf{x}_u), \tag{8}$$

$$\begin{aligned}\sigma(\mathbf{x}_u) &= \alpha P_a(\mathbf{x}_u) + (1-\alpha) P_a(\hat{\mathbf{y}}_u) \\ &= \alpha \frac{\|\mathbf{x}_u\|_\infty^2}{E[\|\mathbf{x}_u\|_2^2]} + (1-\alpha)\frac{\|\hat{\mathbf{y}}_u\|_\infty^2}{E[\|\hat{\mathbf{y}}_u\|_2^2]},\end{aligned} \tag{9}$$

where α is the weighting factor which takes non-negative real value between 0 and 1. If $\alpha = 1$, the proposed system is equivalent to OFDM system using the conventional SLM (i.e., only the peak amplitude of the transmit signal is minimized). On the other hand, if $\alpha = 0$, the proposed system works so as to minimize only the peak amplitude of the received signal. Note that any OFDM systems using SLM need to send side information to the receiver side to enable the receiver to decode original signal. In this paper, we assume that side information on the selected candidate in SLM is perfectly notified to the receiver side [27]†.

4.2 Receiver Signal Processing with Blanking

This subsection explains how impulsive noise blanking is combined with the proposed e-SLM (Fig. 1(b)). The impulsive noise blanking is carried out whenever the measured value $|r(t)|$ exceeds a given noise detection threshold A_{th} as

$$\hat{r}(t) = \begin{cases} 0, & |r(t)| > A_{th}, \\ r(t), & |r(t)| \le A_{th}. \end{cases} \tag{10}$$

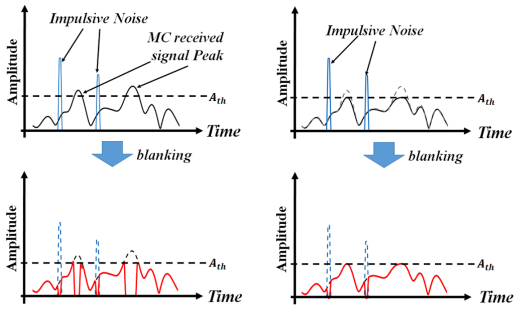

(a) without e-SLM. (b) with e-SLM.

Fig. 4 Effect of deliberate blanking with e-SLM.

Figure 4 illustrates how the proposed e-SLM and blanking jointly work for OFDM-PLC system. When the peak amplitude of the received signal exceeds the blanking threshold A_{th}, the signal amplitude is limited below A_{th} and thus it may degrade the communication quality as in Fig. 4(a). On the other hand, if the e-SLM reduces the received signal peak amplitude below the blanking threshold value A_{th}, impulsive noise is correctly detected by adopting the blanking threshold as in Fig. 4(b).

4.3 Channel Estimation for e-SLM

The proposed e-SLM needs CSI. In this study, we propose iterative channel estimation (CE) method and evaluate the impact of CE error on the achievable performance of eSLM. Let $P(l)$ and $H(l)$ denote pilot signal and frequency response of PLC channel in the l-th subcarrier. Then, the received pilot is given as $R(l) = P(l)H(l) + N(l)$, where $N(l)$ denotes Class-A noise. Channel estimate at the l-th subcarrier frequency $\hat{H}(l)$ is given as

$$\hat{H}(l) = \frac{R(l)}{P(l)} = H(l) + \frac{N(l)}{P(l)}, (l = 1, ..., L). \tag{11}$$

Channel frequency response (CFR) is transformed to channel impulse response (CIR) $\hat{h}(t), (0 \le t \le T_s)$ by IFFT, where $|\hat{h}(t)|$ below a given threshold is replaced with 0. To suppress noise, windowing function is applied to $\hat{h}(t)$ (as shown in Fig. 5), where for simplicity of discussions, we assume that all of the paths are within the GI interval. In this paper, we employ an adaptive windowing algorithm that control length of the window function adaptively to predictive value of CE error. We summarize the adaptive windowing algorithm as follows:

1. First, initial window length is set to be the same as GI length, and compute the CIR $\hat{h}^0(n) = \hat{h}(n)w(n)$, where $w(n)$ given as follows is rectangular window function:

†One of the ways to realize this assumption is to estimate the phase sequence at the receiver side without explicit side information. For example, such SLM methods are investigated in Refs. [28]–[30]. These existing techniques can be also applied to the proposed e-SLM. This means that our proposed method can work with more realistic assumption. Performance evaluation in such cases will be considered for future works.

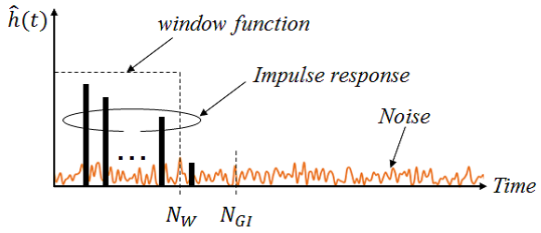

Fig. 5 Illustration of adaptive denoising in channel estimation.

$$w(n) = \begin{cases} 1 & (0 \le n \le N_W) \\ 0 & (n > N_W). \end{cases} \tag{12}$$

N_W and N_{GI} denote the number of sampling points within the window length and GI length. The initial value of estimated CSI $\hat{H}^0(l)$, $(l = 1, ..., L)$ is computed by applying IFFT to $\hat{h}^0(n)$.

2. Set the $N_W = N_{GI} - i, (i = 1, ..., N_{GI})$ and then compute the CIR $\hat{h}^i(t)$, $(i = 1, ..., N_{GI})$ and CSI $\hat{H}^0(l)$, $(l = 1, ..., L)$. Compute the mean square error (MSE) of $\hat{H}^i(l)$ and $\hat{H}^0(l)$ by

$$E(i) = \sum_{l=1}^{L} \left(\hat{H}^i(l) - \hat{H}^0(l)\right)^2 \tag{13}$$

3. Compute the amount of variation of the estimated channel by

$$\Delta E(i) = \left|\frac{E(i+1)}{E(i)}\right|, (i = 1, ..., N_{GI}) \tag{14}$$

4. Finally, select the window length $N_W^o = \max_i\{\Delta E(i)\}$.

In this paper, we assume that estimated CSI is ideally informed to the transmitter side.

5. Performance Evaluation

We evaluate the performance of OFDM-PLC system using the proposed e-SLM by computer simulation. Simulation parameters are summarized in Table 1. The number of subcarriers is set to 64 for mathematical channel model, and 96 for measured channel model. System block diagram is the same as in Fig. 1(a) and the Class-A Middleton noise model is used. We consider two-branch channel model in Fig. 2(a). In addition, as explained in Sect. 3.2.2, we also evaluate performance of OFDM-PLC system with measured channel characteristics in Fig. 3. At the receiver, ADC has finite output range and thus impulsive noise amplitude is limited below V_{max} and dynamic range of ADC is set to D_R = 13 dB. The number of quantization bits is set to 8.

We evaluate the complimentary cumulative distribution function (CCDF) of normalized instantaneous OFDM signal power. Figure 6(a) illustrates CCDF of the instantaneous power of the transmit and receive signals as a function of weighting factor α when CSI is perfectly estimated, where the number of subcarriers is 64. The number of candidate for e-SLM is U=64, where U is empirically determined as

Table 1 Simulation parameters.

Parameters	Value
Number of subcarriers	64, 96
Modulation	QPSK, 16QAM
Number of FFT points	128
l_1, l_2, l_3, l_4, l_5	3m,10m,6m,15m,2m
U	64
Class-A noise parameter	$\Lambda = 0.01, \Gamma = 0.0001$

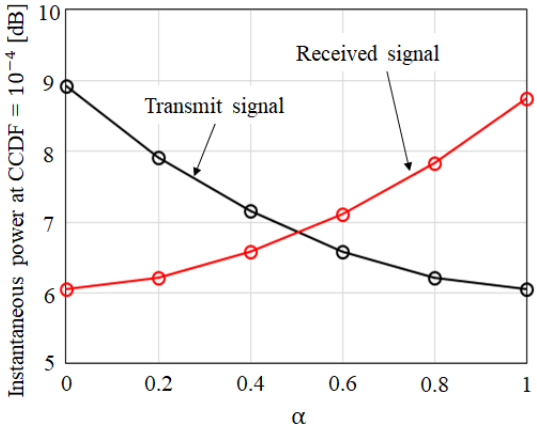

(a) α vs PAPR characteristics ($E_b/N_0 = \infty$) dB.

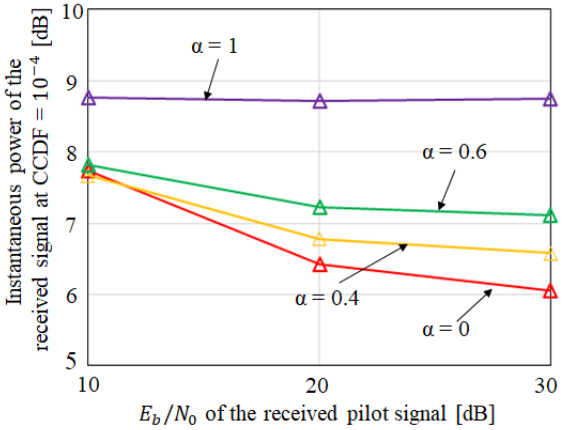

(b) PAPR reduction performance of e-SLM in presence of channel estimation error, where PAPR is defined instantaneous OFDM signal power at CCDF = 10^{-4}.

Fig. 6 PAPR characteristics (U = 64).

a near-optimum value to achieve the trade-off relationship between achieved PAPR and the computational complexity. In Fig. 6(a), the instantaneous powers of the transmit signal and the received signal are normalized by the average power of the transmit signal and the average power of the received signal, respectively. The received signal is not affected by AWGN. Thus average transmit signal power is the same the received one (i.e., the transmit signal and receive signal are normalized by the same reference power)†. From this figure, we can confirm that the PAPR of the transmit signals

†We assume that channel gain is normalized to 1 and thus the average power of the transmit signal is the same as that of the received signal.

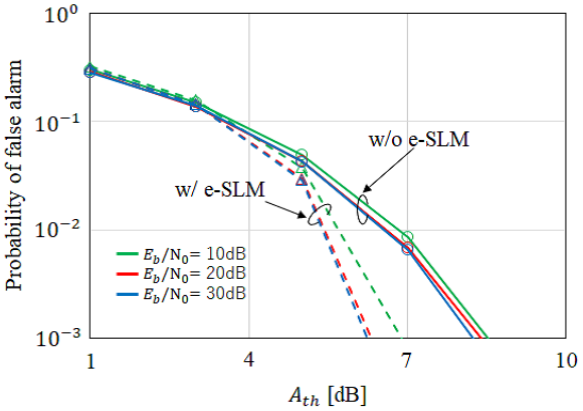

Fig. 7 Probability of false alarm on impulsive noise detection.

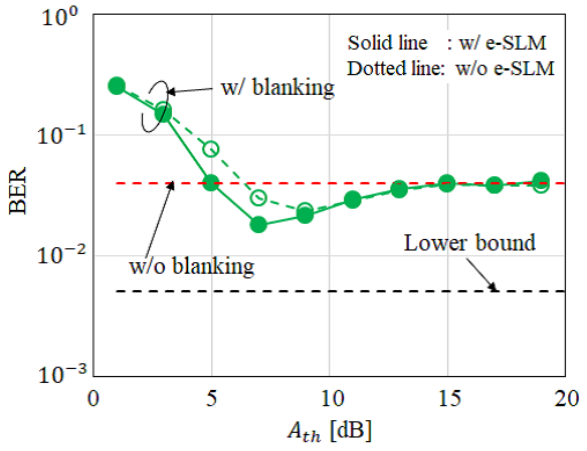

(a) QPSK.

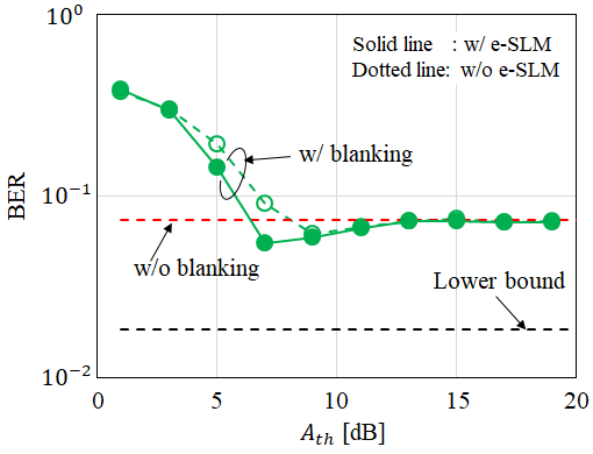

(b) 16QAM.

Fig. 8 Relation between A_{th} and BER (E_b/N_0 = 25 dB, U = 64).

is reduced as α increases, while PAPR of the receive signal is increased as α increases. PAPR of the transmit and received signal are reduced equally when α=0.5 is used in the proposed method. PAPR regrowth of the received signal depends on the channel characteristics. In addition, since nonlinear distortion generated at the transmitter side is dependent on the IBO of the amplifier and nonlinear distortion at the receiver side depends on the blanking threshold, we need to select α by various parameters. This figure suggests that PAPR of both transmit and the receive signals can be controlled by adjusting the value of α.

Figure 6(b) illustrates the relation between E_b/N_0 of the received pilot signal and CCDF of instantaneous power of the received signals using e-SLM under the influence of channel estimation error. Note that PAPR characteristics in Fig. 6(b) represent PAPRs of the actual received signal, not replica at the transmitter. PAPR reduction performance of the received signal is degraded in low E_b/N_0 region because received signal replica is not estimated correctly at the transmitter side due to channel estimation error.

Figure 7 shows probability of false alarm (PoF) of impulsive noise detection at the receiver in OFDM-PLC systems. PoF of impulsive noise is defined as a probability that impulsive noise is erroneously detected at time instance when impulsive noise does not exist. Solid line and dotted line show PoF performance in case without and with the proposed e-SLM, respectively. The noise detection threshold A_{th} is normalized by the average power of the transmit signal, where channel gain is normalized to 1 (i.e., the received signal power is the same as the transmit signal in presence of noise). From this figure, it can be seen that PoF performance is improved by applying the proposed method, because received multi-carrier signal amplitude is reduced below the blanking threshold value.

Figure 8 illustrates the relation between impulsive noise detection threshold A_{th} and BER in absence of nonlinear distortion at PA, where E_b/N_0 = 25 dB. Here, α = 0 and U = 64 are used in the e-SLM. In this figure, the performance of QPSK-OFDM and 16QAM-OFDM is shown, respectively. Dotted line and solid line show the performance with and without the proposed e-SLM, respectively. The label "lower bound" illustrates the case where all impulsive noise is removed perfectly at the receiver side without distorting the received signal. Red line shows the BER performance of the case without the proposed method (w/o PAPR reduction and w/o impulsive noise blanking). From this figure, it can be seen that the proposed e-SLM improves BER performance by mitigating the signal distortion caused by misdetection of impulsive noise. It can be also seen that the proposed e-SLM achieves better BER performance when A_{th} is set to proper level.

Figure 9 shows BER performance of PLC system as a function of the amount of IBO, where U = 64 and A_{th}=7 dB are used. E_b/N_0 is set to 35 dB. In the proposed e-SLM, α is used to jointly control peak power of the transmit signal and that of the received signal. As explained in Sect. 4.1, if α=1, only peak power of the transmit signal is reduced, while only peak power of the received signal is reduced if α =0. Thus, α should be optimized to minimize the BER. From this figure, it can be seen that BER performance is minimized by using α = 0.4 in case of IBO=4 dB. In this paper, we use α=0.4 as an empirically determined optimum value to minimize BER in case of IBO=4 dB. On the other hand, it is also seen that

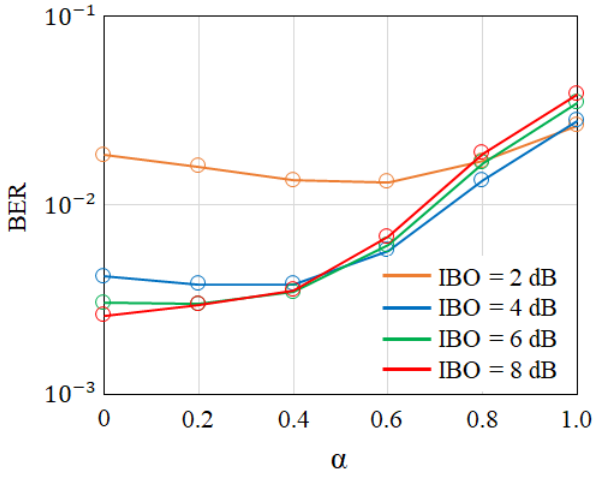

Fig. 9 Relation between α and BER (16QAM, $U = 64$, $A_{th} = 7$ dB).

if IBO is less than 4 dB, the optimum α will be higher than 0.4 to mainly mitigate the influence of nonlinear distortion at the transmitter power amplifier.

Figures 10(a) and 10(b) show BER performance of PLC systems using QPSK-OFDM and 16QAM-OFDM, respectively. Impulsive noise detection threshold is set to $A_{th} = 7$ dB and $U = 64$ is used in e-SLM. Dotted line and solid line show the BER performance with and without the proposed e-SLM. For comparison, we also show the ideal case BER performance (black line) where impulsive noise is perfectly removed without distorting the received signal. Red line shows the case without impulsive noise blanking, which corresponds to $A_{th} = \infty$. Blue line shows the performance of the proposed e-SLM with $\alpha = 1.0$ which corresponds to the conventional SLM (i.e., reducing only PAPR of transmit signal). These figures show that BER performance is improved by both the proposed e-SLM and blanking. Also, it is clear that the proposed method is effective in mitigating the impulsive noise. This is due to the characteristics of the class A noise model used in this paper. Therefore, there is no need to use blanking in high E_b/N_0 region, because the effect of impulsive noise is not dominant. Note that if blanking is not applied to the received signal, BER in low E_b/N_0 region degrades. In addition, although the conventional blanking approach can improve the BER in low E_b/N_0 region, error floor appears due to nonlinear blanking distortion in high E_b/N_0 region, because the high peak amplitude of the received signal causes erroneous detection of the impulsive noise which degrades BER performance. On the other hand, the proposed e-SLM can solve the above problems, simultaneously. This fact implies that overall performance of the proposed method (i.e., e-SLM with blanking) is the best compared with "only blanking" or "without blanking".

To clarify the effect of the adaptive algorithm for channel estimation, the BER performance of PLC-OFDM system with and without the adaptive algorithm over "measured channel II" is evaluated in Fig. 11, where blanking and e-SLM with $\alpha = 0.4$ are adopted. Blanking threshold A_{th} is

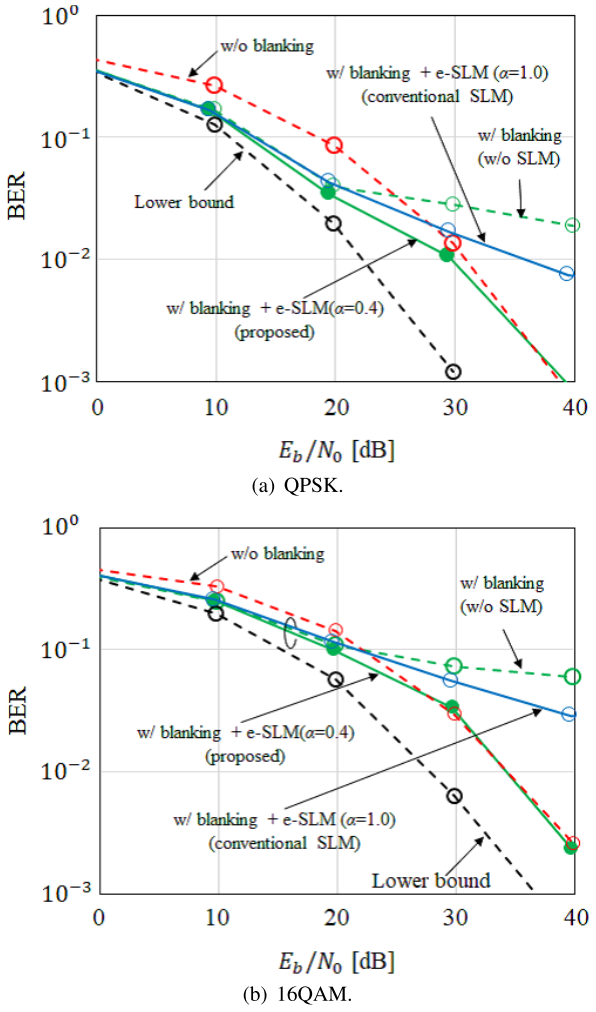

(a) QPSK.

(b) 16QAM.

Fig. 10 BER performance of the proposed method (IBO = 4 dB, $A_{th} = 7$ dB, and $U = 64$).

set to 7 dB. For comparison, fixed windowing sizes and ideal channel estimation cases are also shown. In the fixed windowing, the windowing size in Fig. 5 is fixed to $N_W = 0.2N_{GI}$ and $0.8N_{GI}$, respectively. Note that $N_W = 0.8N_{GI}$ is empirically determined fixed window size which approximately achieves the best BER performance. We assume that signal bandwidth is 6.5 MHz (8.5–15 MHz). The best 96 subcarriers are selected for data transmission according to estimated SNR of each subcarrier. From this figure, we can confirm that the adaptive algorithm shows good BER performance comparable to ideal case. In addition, it is clear that the adaptive algorithm achieve the best BER result compared with the fixed windowing case, because the window size can be adaptively optimized so as to minimize the BER. We have also confirmed effectiveness of the adaptive algorithm over measured channel and mathematical channel model.

To clarify achieved BER of the proposed system in more realistic channel environments, we evaluate the BER performance over measured PLC channels in Fig. 12. The CE in Sect. 4.3 is carried out to estimate CFRs of Fig. 12 and used for estimating the received signal's PAPR at e-SLM. To sim-

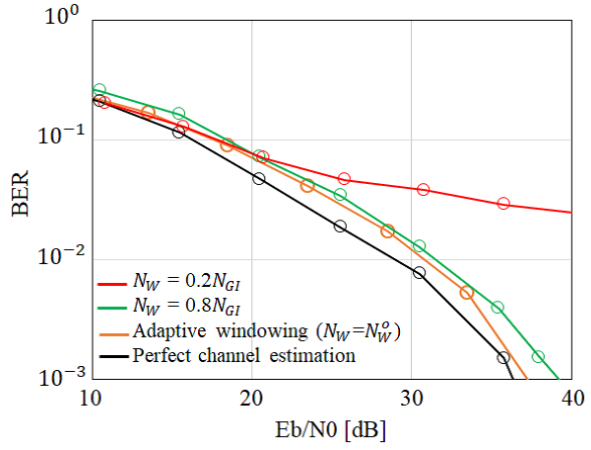

Fig. 11 BER performance using adaptive channel estimation method.

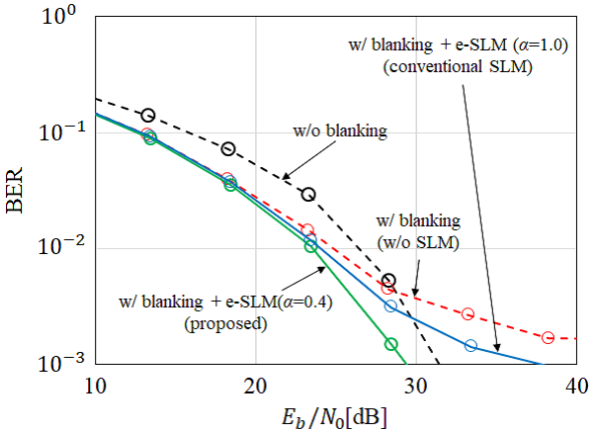

(a) Measured channel I.

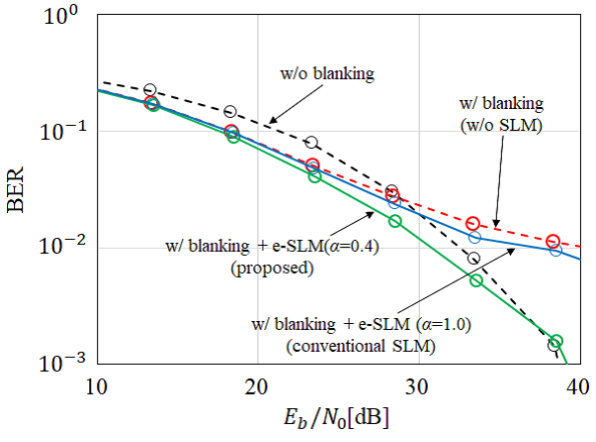

(b) Measured channel II.

Fig. 12 BER in measured PLC channels with adaptive windowing.

plify the discussions, we assume that signal bandwidth is 6.5 MHz, while CE is done for 2-28 MHz in Fig. 12. The best 96 subcarriers are selected for data transmission according to estimated SNR of each subcarrier. Figures 12(a) and 12(b) show the case of measured channel I (15–21.5 MHz) and measured channel II (8.5–15 MHz), respectively. In Fig. 12, black line shows the BER performance of the case without the proposed method (w/o PAPR reduction and impulsive noise blanking). Red line shows the performance of the case without proposed e-SLM. Green and blue lines show the performance in the case with e-SLM when α = 0.4 and α = 1.0 are used, respectively. Here, the case with α=1.0 is equivalent to case with the conventional SLM. From these figures, it can be seen that the proposed e-SLM improves BER performance by mitigating the signal distortion caused by misdetection of impulsive noise over measured PLC channels.

6. Conclusion

In this paper, we have proposed an enhanced SLM method that jointly achieves PAPR reduction on the transmitter side and impulsive noise suppression on the receiver side in OFDM-PLC systems. The proposed method selects the best candidate sequence that minimizes the weighted sum of peak amplitude of transmit signal and the estimated one of the receive signal. Simulation results clarified that the proposed method achieves both the improved BER and the reduced PAPR performance of PLC system.

Acknowledgments

This research was partially supported by the JSPS KAKENHI (JP17K06427, JP17J04710), and the Telecommunications Advancement Foundation.

References

[1] W.Y. Chen, Home Networking Basis: Transmission Environments and Wired/Wireless Protocols, Prentice Hall, 2003.
[2] Y.H. Ma, P.L. So, and E. Gunawan, "Performance analysis of OFDM systems for broadband power line communications under impulsive noise and multipath effects," IEEE Trans. Power Del., vol.20, no.2, pp.674–682, April 2005.
[3] S.A. Bhatti, Q. Shan, I.A. Glover, R. Atkinson, I.E. Portugues, P.J. Moore, and R. Rutherford, "Impulsive noise modeling and prediction of its impact on the performance of WLAN receiver," IEEE 17th European Signal Processing Conference, Glasgow, Scotland, Aug. 2009.
[4] J.T. Gómez, "A survey on impulsive noise modeling," Revista Telemática, vol.16, no.1, pp.101–113, 2017.
[5] K. Khalil, P. Corlay, F. Coudoux, M.G. Gazalet, and M. Gharbi, "Analysis of impact of impulsive, noise parameter on BER performance of OFDM power-line communications," IEEE arXiv: 1502.06821, Feb. 2015.
[6] Y. Rahmatallab, "Peak-to-average power ratio reduction in OFDM systems: A survey and taxonomy," IEEE Commun. Survey Tuts., vol.15, no.4, pp.1567–1592, March 2013.
[7] T. Kageyama, O. Muta, and H. Gacanin, "An enhanced selected mapping technique for joint PAPR reduction and impulsive noise suppression in multi-carrier powerline communications systems," 2018 IEEE International Symposium on Power Line Communications and its Applications, April 2018.
[8] O.P. Haffenden et al., "Detection and removal of clipping in multi-carrier receivers," Eur. Patent Appl., EP1043874, Oct. 2000.
[9] K.S. Vastola, "Threshold detection in narrow-band non-Gaussian noise," IEEE Trans. Commun., vol.COM-32, no.2, pp.134–139, Feb. 1984.

[10] F.H. Juwono, Q. Guo, D. Huang, and K.P. Wong, "Deep clipping for impulsive noise mitigation in OFDM-based power-line communications," IEEE Trans. Power Delivery, vol.29, no.3, pp.1335–1343, June, 2014.
[11] F.H. Juwono, Q. Guo, D. Huang, Y. Chen, L. Xu, and K.P. Wong, "On the performance of blanking nonlinearity in real-valued OFDM based PLC," IEEE Trans. Smart Grid, vol.9, no.1, pp.449–457, Jan. 2018.
[12] Y.R. Chien, "Iterative channel estimation and impulsive noise mitigation algorithm for OFDM-based receivers with application to power-line communications," IEEE Trans. Power Del., vol.30, no.6, pp.2435–2442, Dec. 2015.
[13] K.M. Rabie and E. Alsus, "Effective noise cancellation using single-carrier FDMA transmission in power-line channels," IEEE Trans. Power Del., vol.29, no.5, pp.2110–2117, Oct. 2014.
[14] S.V. Zhidkov, "Performance analysis and optimization of OFDM receiver with blanking nonlinearity in impulsive noise environment," IEEE Trans. Veh. Technol., vol.55, no.1, pp.234–242, Jan. 2006.
[15] S.V. Zhidkov, "Analysis and comparison of several simple impulsive noise mitigation schemes for OFDM receivers," IEEE Trans. Commun., vol.56, no.1, pp.5–9, Jan. 2008.
[16] M. Asadpour, F.A. Ajhiri, B.M. Tazehkand, and M.H. Seyedarabi, "Jointly RVM based channel estimation and PAPR reduction using modified tabu search algoritm in power line communication systems," Wireless Pres. Commun., vol.84, no.4, pp.2757–2775, June, 2015.
[17] K.M. Rabie and E. Alsusa, "Efficient SLM based inpulsive noise reduction in powerline OFDM communication systems," IEEE Global Communications Conference, Dec. 2013.
[18] J.S. Lee, H. Oh, J. Kim, and J.Y. Kim, "Performance of scaled SLM for PAPR reduction of OFDM signal in PLC channels," IEEE International Symposium Power Line Communications and its Applications, Dresden, Germany, Aug. 2009.
[19] K. Anoh, B. Adebisi, K.M. Ravie, M. Hammoudeh, and H. Gacanin, "On companding and optimization of OFDM signals for mitigating impulsive noise in power-line communication systems," IEEE Access, vol.5, pp.21818–21930, 2017.
[20] E.G. Mohammed, B. Jamel, and A. Benbassou, "Peak to average power ration reduction in OFDM system using constant envelope for transmission via PLC channel," Progress in Electromagnetics Research Symposium, Marrakesh, Morocco, March, 2011.
[21] K.M. Rabie, E. Alsusa, and A.D. Familua, "Constant envelope OFDM transmission over impulsive noise power-line communication channels," Proc. IEEE ISPLC, pp.13–18, March 2015.
[22] C.R. Paul, Analysis of Multiconductor Transmission Lines, Wiley-IEEE, 2008.
[23] H. Meng, S. Chen, Y.L. Guan, C.L. Law, P.L. So, E. Gunawan, and T.T. Lie, "A transmission line model for high-frequency power live communication channel," IEEE Int. Conf. on Power Syst. Technol., PowerCon., pp.1290–1298, 2002.
[24] L.T. Berger, and G.M. Rodriguez, "Power line communication channel modelling through concatenated IIR-Filter elements," J. Commun., vol.4, no.1, pp.41–51, Feb. 2009.
[25] D. Middleton, "Canonical and quasi-canonical probability models of class a interference," IEEE Trans. Electromagn. Compat., vol.EMC-25, no.2, pp.76–106, May 1983.
[26] D. Middleton, "Statistical-physical models of electromagnetic interference," IEEE Trans. Electromagn. Compat., vol.EMC-19, no.3, pp.106–127, Aug. 1977.
[27] N. Ohkubo and T. Ohtsuki, "Design critheria for phase sequences in selected mapping," IEICE Trans. Commun., vol.E86-B, no.9, pp.2628–2636, Sept. 2003.
[28] O. Muta, Y. Ohki, and T. Kageyama, "Partial scrambling selected mapping for PAPR reduction of OFDM signals," IEICE Communications Express, vol.6, no.9, pp.535–541, Sept. 2017.
[29] M. Breiling, S.H. Muller, and J.B. Huber, "SLM peak-power reduction without explicit side information," IEEE Commun. Lett., vol.5, no.6, pp.239–241, June 2001.
[30] O. Muta, "Construction and blind estimation of phase sequences for subcarrier-phase control based PAPR reduction in LDPC coded OFDM systems," IEICE Trans. Fundamentals, vol.E93-A, no.11, pp.2130–2140, Nov. 2010.

Tomoya Kageyama received B.E. degree and M.E. degree from Kyushu University, Japan, in 2015 and 2017, respectively. Presently, he is a doctoral student at Kyushu University, Japan. His research interests include PHY layer signal processing techniques for powerline communications and MIMO wireless communications.

Osamu Muta received B.E. degree from Ehime University, in 1996, M.E. degree from Kyushu Institute of Technology, Japan, in 1998, and Ph.D. degree from Kyushu University in 2001. In 2001, he joined the Graduate School of Information Science and Electrical Engineering, Kyushu University as an assistant professor. Since 2010, he has been an associate professor in Center for Japan-Egypt Cooperation in Science and Technology, Kyushu University. His current research interests include signal processing techniques for wireless communications and powerline communications, MIMO, and nonlinear distortion compensation techniques for high-power amplifiers. He received the 2005 Active Research Award from IEICE technical committee of radio communication systems, the 2014, the 2015, and the 2017 Chairman's Awards for excellent research from IEICE technical committee of communication systems, respectively. Dr. Muta is a member of IEEE.

Haris Gacanin received his M.E.E. and Ph.D.E.E. from Graduate School of Electrical Engineering, Tohoku University, Japan, in 2005 and 2008, respectively. Since April 2008 until May 2010 he has been working first as Japan Society for Promotion of Science (JSPS) postdoctoral research fellow and then as an Assistant Professor at Graduate School of Engineering, Tohoku University. Currently, he is with Nokia, Belgium. His research interest is in the fields of wireline and wireless communications with focus on wireless network coding, channel estimation and equalization, cognitive radio, MIMO, wireless sensor networks, dynamic resource allocation, iterative receivers. He is member of IEEE and senior member of IEICE and was Chair of the IEICE Europe Section. He is a recipient of the 2010 KDDI Foundation Research Grant Award, the 2008 Japan Society for Promotion of Science (JSPS) Postdoctoral Fellowships for Foreign Researchers.